Influence of Metallocene Type on the Order of Ethylene Polymerization and Catalyst Deactivation Rate in a Solution Reactor

*Saeid Mehdiabadi, João B.P. Soares**

Summary: The solution polymerization of ethylene using rac-Et(Ind)$_2$ZrCl$_2$/MAO and (Dimethylsilyl(tert-butylamido)(tetramethyl- cyclopentadienyl)titanium Dichloride)(CGC-Ti)/MAO was studied in a semi-batch reactor at 120 °C under different monomer pressures and catalyst concentrations. The kinetics of ethylene polymerization with rac-Et(Ind)$_2$ZrCl$_2$/MAO can be described with first order reactions for polymerization and catalyst deactivation. When (CGC-Ti)/MAO is used, however, second order kinetics are observed for catalyst decay and the order of polymerization changes from 2 to 1 with increasing ethylene pressure.

Keywords: metallocene catalysts; polyethylene; polymerization kinetics; solution polymerization; polymerization reaction engineering

Introduction

The use of two single-site catalysts to synthesize polymers with complex microstructures is a very promising way to create novel polyolefins. For instance, dual metallocene systems have been used to produce polyolefins with bimodal distributions of molecular weight[1] and chemical composition,[2] and to maximize the formation of long chain branches in polyethylene.[3] Dual single-site catalysts have also been used to produce branched[4,5] and linear[6] olefin block copolymers.

These techniques require a detailed knowledge of the kinetics of polymerization of both catalysts in order to make polymers with the proper balance of the two components. For instance, a polyolefin with bimodal molecular weight distribution will be produced only if the mass fractions and ratios of molecular weight averages of the polymers made by the two catalysts are within a specified range.[7] Since these variables are sensitive to polymerization temperature, monomer pressure, catalyst and hydrogen concentrations, a polymerization kinetic model is essential for the control of the properties of polymers made with dual single-site catalysts.

In this article, we investigate how polymerization conditions in a solution reactor affect the polymerization kinetics of two metallocene catalysts, rac-Et(Ind)$_2$ZrCl$_2$ and the constrained geometry catalyst (CGC-Ti).

Experimental

Materials

Methylaluminoxane (MAO, 10 wt % in toluene, Sigma-Aldrich) was used as received. Ethylene and nitrogen (Praxair) were purified by passing through molecular sieves (3 and 4-Å) and copper(II)oxide packed beds. Toluene (EMD) was purified by distillation over a n-butyllithium/styrene/sodium system and then passed through two packed columns in series filled with molecular sieves (3, 4, and 5-Å) and Selexorb for further purification. All air-sensitive compounds were handled under inert atmosphere in a glove box.

The catalyst rac-ethenebis(indenyl) zirconium dichloride (rac-Et[Ind]$_2$ZrCl$_2$) and CGC-Ti were purchased as powder from

Department of Chemical Engineering, University of Waterloo, Waterloo, Ontario, Canada N2L 3G1
E-mail: jsoares@uwaterloo.ca

Sigma-Aldrich and Boulder Scientific respectively and were dissolved in distilled and molecular sieve passed toluene at concentrations of 1×10^{-8} and 4×10^{-7} mol/g before polymerization.

Polymer Synthesis

All polymerizations were performed in a 500 ml Parr autoclave reactor operated in semi-batch mode. The polymerization temperature was controlled using an electrical band heater and internal cooling coils. The reaction medium was mixed using a pitched-blade impeller connected to magneto-driver stirrer, rotating at 2000 rpm. Prior to use, the reactor was heated to 125 °C, evacuated, and refilled with nitrogen six times to reduce the oxygen level in the reactor, before being charged with 250 ml of toluene and 0.5 g of $AliBu_3$ as a scavenger. The temperature was then increased to 120 °C and kept constant for 20 minutes. Finally, the reactor contents were blown out under nitrogen pressure. This procedure ensures excellent removal of impurities from the reactor walls.

In a typical polymerization run, 200 ml of toluene were charged into the reactor, followed by an appropriate amount of MAO, introduced via a 5 ml tube and a 20 ml sampling cylinder connected in series with an ethylene pressure differential of 20 psig. A specified volume of toluene was placed in the sampling cylinder before injection to wash the tube wall from any MAO solution. The same method was applied to inject the catalyst solution into the reactor. Monomer was supplied on demand to maintain a constant reactor pressure of 120 psig and monitored with a mass flow meter. With the exception of a 1–2 °C exotherm upon catalyst injection, the temperature was kept at 120 °C ± 0.15 °C throughout the reaction. After 15 minutes, the polymerization was stopped by closing the monomer valve and immediately blowing out the reactor contents into a 1-L beaker filled with 400 ml of ethanol. The polymer produced was then kept overnight, filtered, washed with ethanol, dried in air, and further dried under vacuum.

Polymer Characterization

Molecular weight distributions (MWD) were determined with a Polymer Char high-temperature gel permeation chromatographer (GPC), at 145 °C under a flow rate of trichlorobenzene of 1 ml/min. Our GPC is equipped with three detectors in series (infra-red, light scattering and differential viscosimeter). The GPC was calibrated with polystyrene narrow standards.

Results and Discussion

rac-Et(Ind)$_2$ZrCl$_2$: Effect of Catalyst Concentration

A complete randomized design with seven catalyst concentration levels and two replicates at each level was used to investigate the kinetics of rac-Et(Ind)$_2$ZrCl$_2$ deactivation. All polymerizations were performed at 120 °C and 120 psig ethylene pressure with the same volume of solvent (222.8 ml toluene) and mass of MAO (1.6258 g). Figure 1 shows the ethylene volumetric consumption rates versus polymerization time for these set of runs.

Several elementary reactions take place during coordination polymerization: initiation, propagation, long chain branch formation, transfer reactions, and deactivation. For catalyst deactivation studies, however, just the initiation, propagation and deactivation steps need to be considered, as described below,

$$\textit{Initiation} \quad C_i + M \xrightarrow{k_p} P^* \tag{1}$$

$$\textit{Propagation} \quad P^* + M \xrightarrow{k_p} P^* \tag{2}$$

$$\textit{Deactivation} \quad P^* \xrightarrow{k_d} D + \hat{C}_i \tag{3}$$

$$C_i \xrightarrow{k_d} \hat{C}_i \tag{4}$$

where, P^* represent living chains, D dead chains, C_i, monomer-free active sites, and $\hat{C}_i$ deactivated catalyst sites. We have also assumed that the initiation and propagation constants, k_p, have the same value and that the two catalyst deactivation steps, shown in Equations (3) and (4), also share the same kinetic constant, k_d.

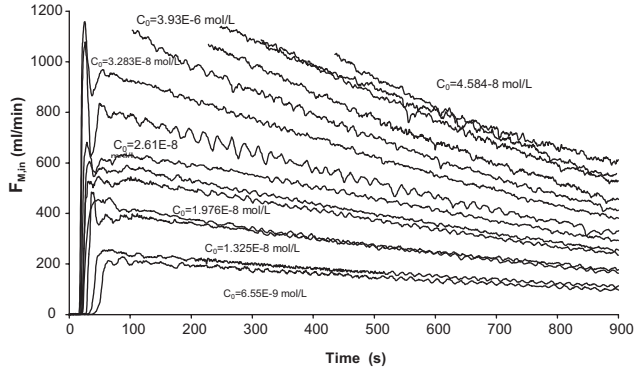

Figure 1.
Ethylene consumption rates (ml/min) versus polymerization time for different catalyst concentrations (C_0).

The molar balances for active catalyst sites and living chains are given by:

$$\frac{d[C_i]}{dt} = -k_p[C_i][M] - k_d[C_i] \quad (5)$$

$$\frac{d[P^*]}{dt} = k_p[C_i][M] - k_d[P^*] \quad (6)$$

Solving these simultaneous differential equations with the initial conditions (at $t=0$) $[C_i] = [C_i]_0$ and $[P^*] = 0$ yields:

$$[P^*] = [C_i]_0[e^{-k_d t} - e^{-(k_d + k_p[M])t}] \quad (7)$$

$$[C_i] = [C_i]_0 e^{-k_d t} - [P^*] \quad (8)$$

The second exponential term in Equation (7) is negligible because it contains the large term $k_p[M]$. Thus, Equation (7) simplifies to:

$$[P^*] = [C_i]_0 e^{-k_d t} \quad (9)$$

The molar balance for monomer is given by

$$\frac{d[M]}{dt} = \frac{F_{M,in}}{V_R} - k_p[P^*][M] \quad (10)$$

where $F_{M,in}$ is the molar flow rate of ethylene to the reactor and V_R is the volume of the reaction medium.

Substituting Equation (9) into Equation (10) and solving the resulting equation using the assumption that monomer concentration is constant, we conclude that, for a first order catalyst decay, the kinetic data has to obey the following relation:

$$\ln\left(\frac{F_{M,in}}{V_R}\right) = \ln(k_p[C_i]_0[M]) - k_d t \quad (11)$$

Consequently, a plot of $\ln\left(\frac{F_{M,in}}{V_R}\right)$ versus time should have a constant slope equal to $-k_d$ and an intercept equal to $\ln(k_p[C_i]_0[M])$ for catalysts that follow first order catalyst decay kinetics and first order propagation rate with respect to monomer concentration. This is exactly what is illustrated in Figure 2 for ethylene polymerization runs with rac-Et(Ind)$_2$ZrCl$_2$. Table 1 shows the values estimated for k_d and $k_p[M]$ under these conditions, as well as the experimental values for polymer yield.

We can describe the values estimated for k_d and k_p with the single-factor ANOVA model,

$$Y_{i,j} = \mu + \tau_i + \varepsilon_{i,j} \quad (12)$$

where $Y_{i,j}$ is the $i \times j^{\text{th}}$ measurement, μ is the overall mean, τ_i is a parameter associated with the i^{th} treatment level (called the treatment effect, in the present case, catalyst concentration) and $\varepsilon_{i,j}$ is a random error component arising from all sources of variability. The null hypothesis is $H_0 : \tau_1 = \tau_2 = \ldots \tau_n = 0$ (where $n = 7$ catalyst concentrations) and the alternative hypothesis is $H_1 : \tau_i \neq 0$ for at least one value of i.

The analysis of variance for the parameter k_d is summarized in Table 2. The test statistic F_0, which is the ratio of treatment

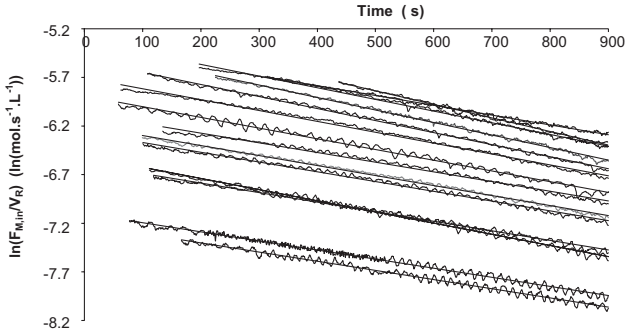

Figure 2.
Ethylene polymerization with rac-Et(Ind)$_2$ZrCl$_2$ under several catalysts concentrations (see Figure 1).

mean square to error mean square was used to test the null hypothesis. Since $F_0 = 2.02$ is less than $F_{0.05\,6,\,7} = 3.866$, we accept the null hypothesis. This means that each k_d measurement consists of the overall mean plus a realization of the random error component $\varepsilon_{i,j}$ or, in other words, it is equivalent to saying that all 14 k_d estimates are taken from a normal distribution with mean μ and variance σ^2. Consequently, catalyst concentration does not influence the value of k_d. The normal probability plot for k_d, shown in Figure 3, confirms the normal distribution of the k_d estimates with confidence level of 95% with a value of $k_d = 1.117 \times 10^{-3} \pm 7.54 \times 10^{-5}\,s^{-1}$.

A similar analysis of variance, repeated for k_p (Table 3), shows that the values estimated for $k_p[M]$ $(1.11 \times 10^5 \pm 6.25 \times 10^3\,s^{-1})$ are also independent of catalyst concentration. The normal probability plot for $k_p[M]$ is shown in Figure 4.

The use of analysis of variance to test for no difference in treatment means requires that the measurement errors be normally and independently distributed with mean

Table 1.
Summary of reaction rate constant calculations for rac-Et(Ind)$_2$ZrCl$_2$ (varying catalyst concentration).

Run	Catalyst conc. mol/L	slope	intercept	$k_p[M]$ (s^{-1})	k_d (s^{-1})	Polymer Yield (g)
8	2.62E-08	−0.00102	−6.05543	8.94×10^3	1.02×10^{-3}	8.60
4	1.97E-08	−0.00104	−6.24759	9.83×10^3	1.04×10^{-3}	7.15
14	4.59E-08	−0.00119	−5.33151	1.05×10^3	1.19×10^{-3}	16.20
3	3.28E-08	−0.00116	−5.67598	1.05×10^3	1.16×10^{-3}	11.74
11	1.33E-08	−0.001	−6.57702	1.05×10^3	1.00×10^{-3}	5.17
12	3.93E-08	−0.00129	−5.39051	1.16×10^3	1.29×10^{-3}	14.36
6	2.60E-08	−0.00114	−5.86786	1.09×10^3	1.14×10^{-3}	9.78
7	1.98E-08	−0.00105	−6.18042	1.05×10^3	1.05×10^{-3}	7.45
1	1.32E-08	−0.00116	−6.50186	1.14×10^3	1.16×10^{-3}	5.32
9	6.53E-09	−0.00098	−7.19717	1.15×10^3	0.98×10^{-3}	2.91
11	4.58E-08	−0.00139	−5.1405	1.28×10^3	1.39×10^{-3}	17.37
2	3.29E-08	−0.00124	−5.52014	1.22×10^3	1.24×10^{-3}	13.10
5	6.53E-09	−0.00095	−7.0934	1.27×10^3	0.95×10^{-3}	3.25
13	3.93E-08	−0.00101	−5.38016	1.17×10^3	1.01×10^{-3}	15.18

Table 2.
Analysis of variance for k_d (varying catalyst concentration).

Source of Variation	Sum of Squares	Degrees of Freedom	Mean Square	F_0	P-Value
Catalyst Concentration	1.40×10^{-7}	6	2.33×10^{-8}	2.02	0.19
Error	8.08×10^{-8}	7	1.15×10^{-8}		
Total	2.21×10^{-7}	13			

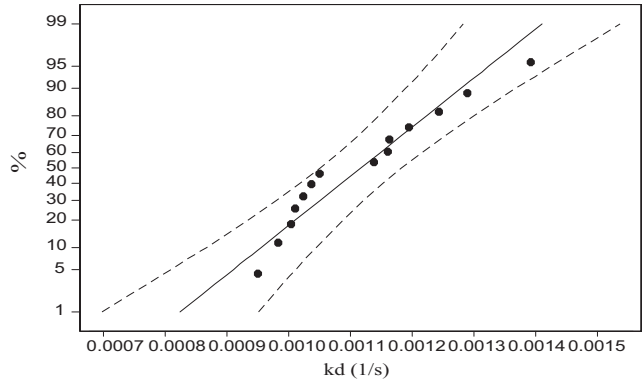

Figure 3.
Normal probability plot for k_d with 95% confidence limits (varying catalyst concentration).

zero and a constant (but unknown) variance σ^2.[8] In Figure 5, the normal probability plot for the residuals of k_d was constructed, indicating that they are normally distributed. No pattern was also seen in the plot of residuals versus run order and concentration, confirming independent distribution of the residuals. The same test was repeated for k_p[M] to test normal distribution of the residuals, as shown in Figure 6.

Estimates for k_p and k_d can also be obtained by computing the mass of polymer (m_p) produced as a function catalyst concentration:

$$m_p = \left(28\frac{\text{g}}{\text{mol}}\right) \times \int_0^t F_{M,in}\,\text{d}t \tag{15}$$

Substituting Equation (11) into Equation (15), we find:

$$m_p = 28\frac{k_p}{k_d}V_R[M](1 - e^{-k_d t})[C_i]_0 \tag{16}$$

Therefore, a plot of polymer yield (m_p) versus catalyst concentration should be

Table 3.
Analysis of variance for k_p[M] (varying catalyst concentration).

Source of Variation	Sum of Squares	Degrees of Freedom	Mean Square	F_o	*P*-value
Catalyst Concentration	7.96×10^8	6	1.33×10^8	1.28	0.38
Error	7.28×10^8	7	1.04×10^8		
Total	1.52×10^9	13			

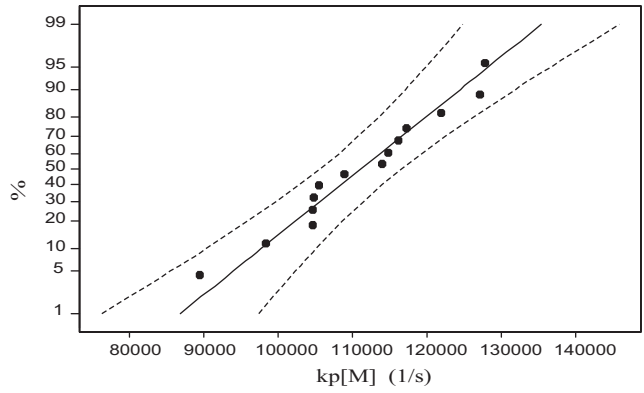

Figure 4.
Normal probability plot for k_p [M] with 95% confidence limits (varying catalyst concentration).

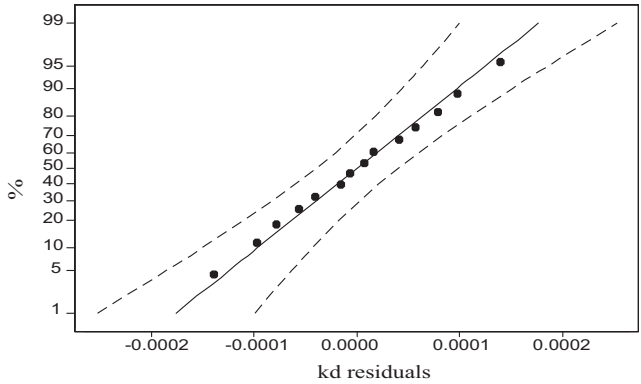

Figure 5.
Normal probability plot for the residuals of k_d (varying catalyst concentration).

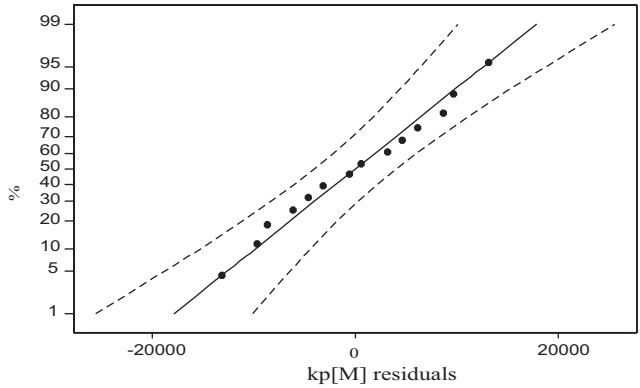

Figure 6.
Normal probability plot for the residuals of k_p[M] (varying catalyst concentration).

linear with a slope $28k_pV_R[M](1-e^{-k_dt})/k_d$, as confirmed in Figure 7. If we estimate the value of $k_p[M]$ from the slope of Figure 7 and the previously estimated value of k_d, we obtain $k_p[M] = 1.05 \times 10^5$, which is in good agreement with the value estimated above using the ANOVA table ($1.11 \times 10^5 \pm 6.25 \times 10^3\,s^{-1}$).

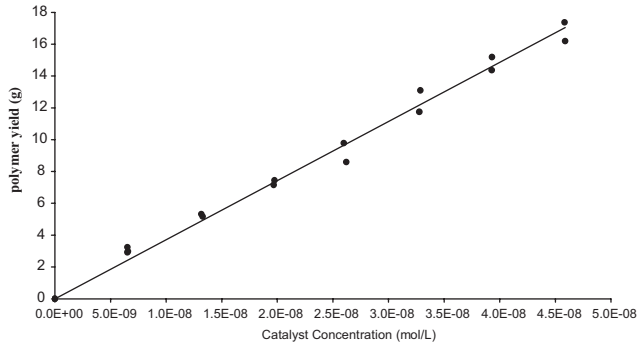

Figure 7.
Polymer yield versus catalyst concentration.

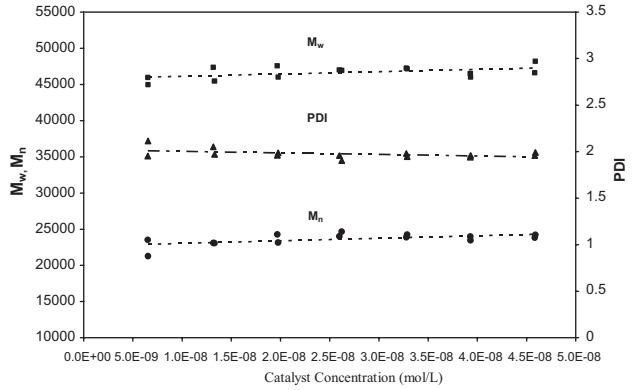

Figure 8.
Molecular weight averages and *PDI* versus catalyst concentration.

It is also interesting to observe that the number and weight average molecular weights (M_n and M_w), as well as the polydispersity index (*PDI*), do not vary as a function of catalyst concentration, as shown in Figure 8.

Rac-Et(Ind)$_2$ZrCl$_2$: Effect of Ethylene Pressure

A complete randomized design with 9 different ethylene pressure levels and two replicates at each level was chosen to test the effect of monomer pressure on polymer yield, molecular weight, and reaction rate constants.

Figure 9 shows the plot of monomer consumption versus time for several ethylene pressures. Similarly to the treatment adopted in Figure 2, we plotted $\ln\left(\frac{F_{M,in}}{V_R}\right)$ versus time in Figure 10 and estimated k_d and $k_p[M]$ from the curves intercepts and slopes. Table 4 summarizes the results of these calculations.

Table 5 gives the analysis of variance for k_d. Since $F_0 = 0.71$ is less than $F_{0.05\ 8,\ 9} = 3.23$, we can conclude that k_d is not affected by monomer pressure.

The normal probability plot for k_d, shown in Figure 11, confirms the normal distribution of the k_d estimates with confidence level of 95% ($k_d = 9.6 \times 10^{-4} \pm 2.22 \times 10^{-5}\,s^{-1}$).

When we compare the value of k_d estimated in Figure 11 ($k_d = 9.6 \times 10^{-4} \pm$

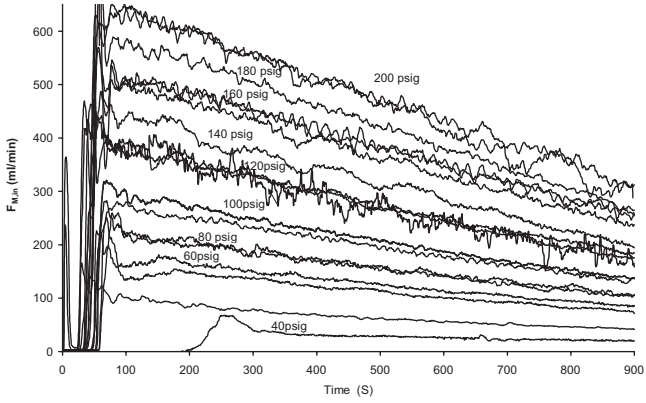

Figure 9.
Ethylene consumption rate (ml/min) versus polymerization time for different ethylene pressures. (The numbers over the curves refer to total pressures at which polymerization were performed).

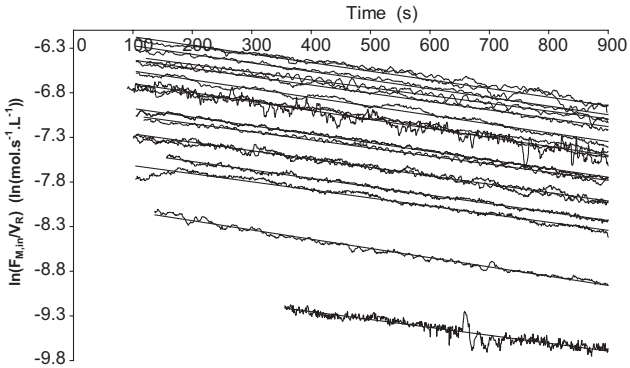

Figure 10.
Ethylene polymerization with rac-Et(Ind)$_2$ZrCl$_2$ under several ethylene pressures (see Figure 9).

$2.22 \times 10^{-5}\,s^{-1}$) with the one estimated in Figure 3 ($1.117 \times 10^{-3} \pm 7.54 \times 10^{-5}\,s^{-1}$) we notice that they disagree slightly. The difference between the sample mean for k_d estimated when the catalyst concentration was changed ($k_{d,C}$) and the one obtained when pressure was varied ($k_{d,P}$) can be better quantified using basic statistics: the 95% confidence interval of the difference between the means is $7.9 \times 10^{-5} \leq k_{d,C} - k_{d,P} \leq 2.3 \times 10^{-4}\,s^{-1}$. This difference is small and may be associated to

Table 4.
Summary of reaction rate constant calculations for rac-Et(Ind)$_2$ZrCl$_2$ (varying ethylene pressure).

Pressure (psig)	Abs. Pressure (psig)	Slope	Intercept	$k_p[M]$ (s^{-1})	k_d (s^{-1})
121.2	135.9	-1.00×10^{-3}	−6.596	1.04×10^{5}	1.00×10^{-3}
140.6	155.3	-9.97×10^{-4}	−6.453	1.20×10^{5}	9.97×10^{-4}
60.3	75.0	-9.75×10^{-4}	−7.481	4.30×10^{4}	9.75×10^{-4}
160.0	174.7	-9.34×10^{-4}	−6.339	1.34×10^{5}	9.34×10^{-4}
200.7	215.4	-9.94×10^{-4}	−6.058	1.77×10^{5}	9.94×10^{-4}
80.4	95.1	-9.40×10^{-4}	−7.167	5.85×10^{4}	9.40×10^{-4}
180.1	194.8	-9.96×10^{-4}	−6.157	1.62×10^{5}	9.96×10^{-4}
100.1	114.8	-9.81×10^{-4}	−6.868	7.89×10^{4}	9.81×10^{-4}
180.4	195.1	-9.24×10^{-4}	−6.288	1.41×10^{5}	9.24×10^{-4}
80.6	95.3	-9.39×10^{-4}	−7.172	5.80×10^{4}	9.39×10^{-4}
140.3	155.0	-9.37×10^{-4}	−6.607	1.03×10^{5}	9.37×10^{-4}
60.8	75.5	-9.45×10^{-4}	−7.381	4.74×10^{4}	9.45×10^{-4}
160.1	174.8	-8.82×10^{-4}	−6.302	1.39×10^{5}	8.82×10^{-4}
99.5	114.2	-9.36×10^{-4}	−6.946	7.29×10^{4}	9.36×10^{-4}
119.8	134.5	-1.02×10^{-3}	−6.602	1.03×10^{5}	1.02×10^{-4}
200.2	214.9	-9.09×10^{-4}	−6.087	1.73×10^{5}	9.09×10^{-4}
39.4	54.1	-9.09×10^{-4}	−8.883	1.06×10^{4}	9.09×10^{-4}
37.8	52.5	-1.05×10^{-3}	−8.021	2.50×10^{4}	1.05×10^{-4}

Catalyst concentration = 1.31×10^{-8}mol/L; Polymerization temperature = 120 °C

Table 5.
Analysis of variance for k_d (varying ethylene pressure).

Source of Variation	Sum of Squares	Degrees of Freedom	Mean Square	F_o	*P*-value
Monomer Concentration	1.31×10^{-8}	8	1.64×10^{-9}	0.71	0.68
Error	2.07×10^{-8}	9	2.30×10^{-9}		
Total	3.38×10^{-8}	17			

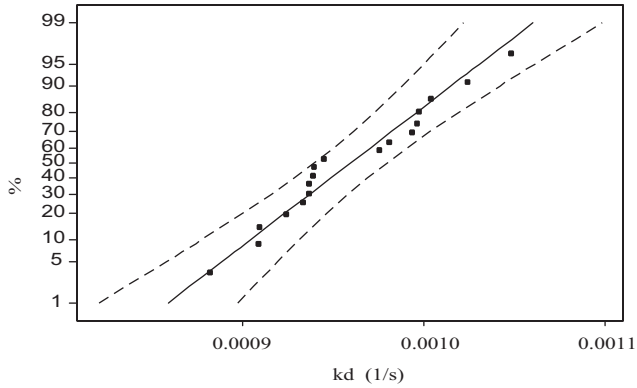

Figure 11.
Normal probability plot for k_d with 95% confidence limit 95% (varying ethylene pressure).

batch-to-batch solvent purity variation, since we used two different solvent batches for the catalyst concentration and ethylene pressure investigations.

The dependencies of $k_p[M]$ on total reactor pressure and ethylene concentration in toluene are shown in Figures 12 and 13, respectively. A clear first order

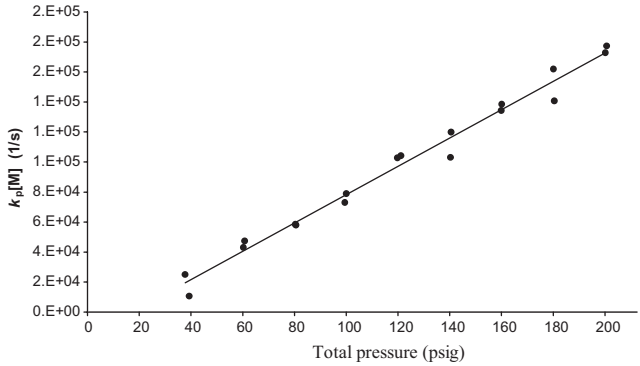

Figure 12.
Plot of $k_p[M]$ versus total pressure.

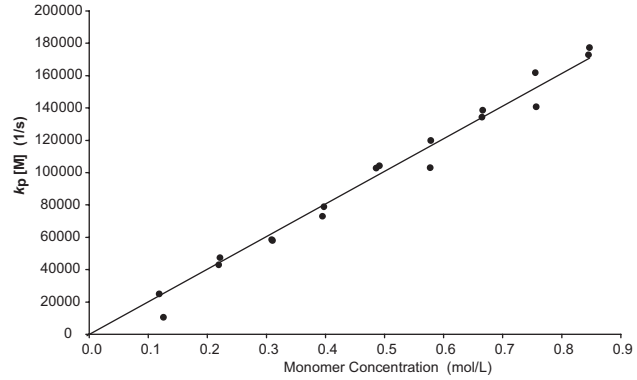

Figure 13.
Plot of $k_p[M]$ versus monomer concentration, estimated using equilibrium data from Lee et al.[9]

Table 6.
Analysis of variance M_w (varying ethylene pressure).

Source of Variation	Sum of Squares	Degrees of Freedom	Mean Square	F_o	*P*-value
Monomer Concentration	2.977×10^7	7	4.253×10^6	7.56	0.008
Error	3.937×10^6	7	5.625×10^5		
Total	3.371×10^7	14			

Table 7.
Analysis of variance M_n (varying ethylene pressure).

Source of Variation	Sum of Squares	Degree of freedom	Mean Square	F_o	*P*-value
Monomer Concentration	1.462×10^7	7	2.089×10^6	4.8	0.028
Error	3.059×10^6	7	4.370×10^5		
Total	1.768×10^7	14			

dependency with respect to ethylene concentration is noticed, and the slope of the curve in Figure 13 gives a point estimate of $k_p = 2.02 \times 10^5\,\mathrm{L \cdot mol^{-1} \cdot s^{-1}}$. (Ethylene concentrations in toluene were calculated using the equilibrium data published by Lee et al.[9]).

The analysis of variance for M_w and M_n is summarized in Tables 6 and 7. Since $F_0 = 7.56$ for M_w and $F_0 = 4.8$ for M_n are both greater than $F_{0.05\ 7,\ 7} = 3.79$, we accept that M_w and M_n are affected by the monomer concentration, as expected. As shown in Figure 14, both M_w and M_n increase linearly with pressure, but the increase in M_w is more pronounced than the increase in M_n, as implied by their *P* and F_0 values.

Figures 15 and 16 show how the polymer yields varies with reactor pressure and ethylene concentration, respectively. These linear relationships confirm again that the rate of polymerization is first order with respect to ethylene concentration for $Et(Ind)_2ZrCl_2$ under this range of experimental conditions.

CGC-Ti Catalyst: Effect of Ethylene Pressure

The effect of ethylene pressure on CGC-Ti polymerization was investigated by varying the reactor pressure from 25 to 220 psig at a constant temperature of 120 °C. First, we analyzed the ethylene consumption rate curves with first and second order catalyst decay models. The first order catalyst decay model has been already described with Equation (11). However, this model fails to describe the polymerization data with CGC-Ti adequately, as shown in Figure 17 for a typical polymerization run.

As an alternative to the first order catalyst decay model, we proposed a second

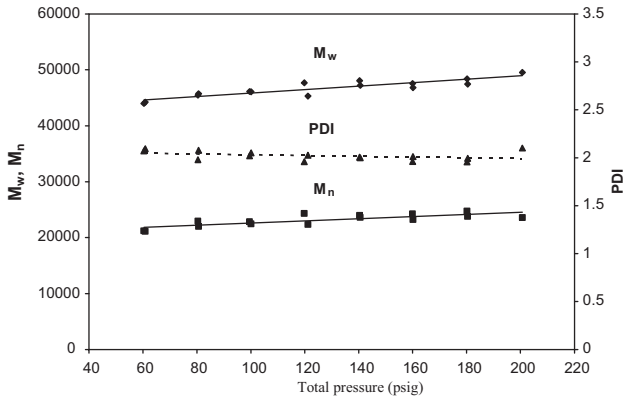

Figure 14.
Effect of ethylene pressure on M_w, M_n and *PDI*.

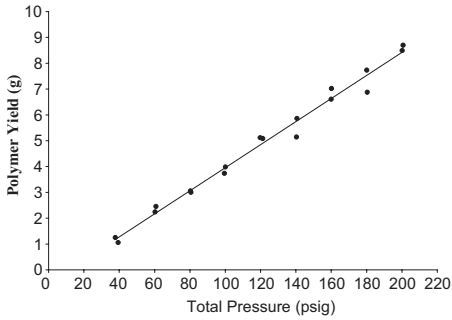

Figure 15.
Polymer yields as a function of total reactor pressure.

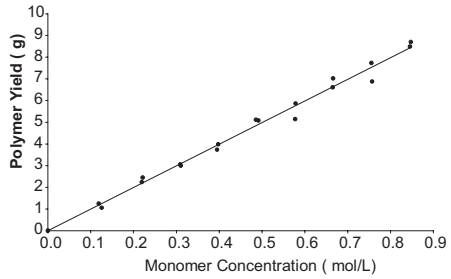

Figure 16.
Polymer yield as a function of ethylene concentration in toluene, estimated using equilibrium data from Lee et al.[9]

order model assuming that the initiation step, Equation (1), was very fast:

$$\frac{\mathrm{d}[C_i]}{\mathrm{d}t} = -k_d[C_i]^2 \tag{17}$$

Following a similar derivation to the one applied for $Et(Ind)_2ZrCl_2$, we finally obtain the following expression:

$$\left(\frac{V_R}{F_{M,in}}\right) = \frac{k_d}{k_p[M]}t + \frac{1}{k_p[M][C_0]} \tag{18}$$

The second order model describes well the polymerization data with CGC-Ti for a wide range of pressures, as illustrated in Figure 18.

Interestingly, the order of propagation with respect to ethylene concentration is not unity for the whole range of ethylene pressures investigated. Figure 19 shows that when the polymer yield is plotted versus reactor pressure a curvature is observed for low pressures. On the other hand, when we plot polymer yield versus the square of the reactor pressure for the low pressure range from 25 to 100 psig (Figure 20), a linear relation is clearly observed, confirming a second order dependency on ethylene pressure (or concentration). Finally, Figure 21 confirms that first order propagation is obeyed in the pressure range from 60 to 220 psig.

This change in propagation order can be explained by the following mechanism,

$$P^* + M \underset{k_r}{\overset{k_f}{\rightleftharpoons}} P^* \cdot M \tag{19}$$

$$P^* \cdot M + M \xrightarrow{k_p} P^* + M \tag{20}$$

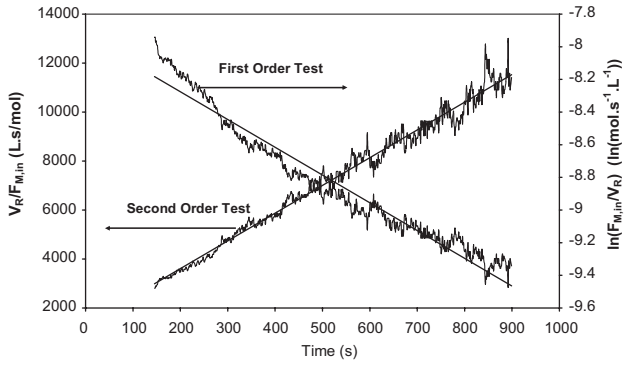

Figure 17.
Test for the first and second order catalyst deactivation with CGC-Ti. (CCG-Ti concentration = 5.47×10^{-7} mol/L; solvent volume = 222.8 ml, mass of MAO = 2 g).

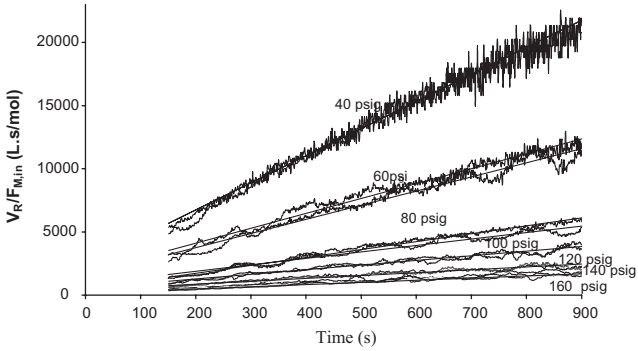

Figure 18.
Ethylene polymerization kinetics with CGC-Ti, indicating second order catalyst deactivation. (CCG concentration = 5.47×10^{-7} mol/L; solvent volume = 222.8 ml, mass of MAO = 2 g).

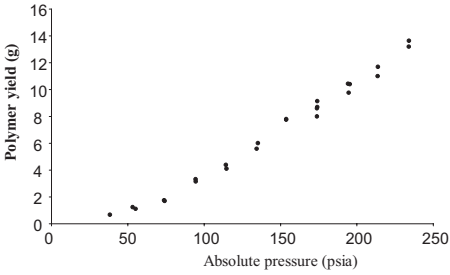

Figure 19.
Polymer yield versus reactor pressure.

which is consistent with the main assumptions of the trigger mechanism.[10]

Applying the steady-state approximation to calculate the concentration of the intermediate species, $P^{*} \cdot M$, we get:

$$[P^{*} \cdot M] = \frac{k_f[M][P^{*}]}{k_r + k_p[M]} \tag{21}$$

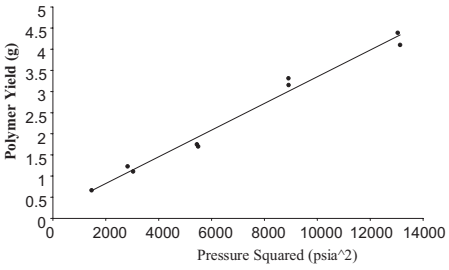

Figure 20.
Polymer yield versus reactor pressure squared, confirming second order propagation order at low ethylene pressure.

Finally, using Equation (21) to calculate the rate of polymerization according to Equation (20), the following expression is derived:

$$R_p = \frac{k_p k_f [P^{*}][M]^2}{k_r + k_p[M]} \tag{22}$$

At low ethylene pressure ($k_p[M] << k_r$), Equation (22) becomes,

$$R_p = \frac{k_p k_f [M]^2 [P^{*}]}{k_r} \tag{23}$$

and the polymerization order with respect to ethylene concentration approaches two.

On the other hand, at high pressures ($k_p[M] >> k_r$), Equation (22) simplifies to,

$$R_p = k_f[M][P^{*}] \tag{24}$$

and first order propagation behaviour is observed. This behaviour agrees well with

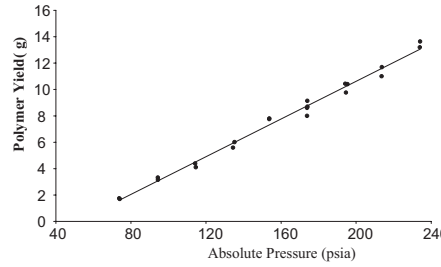

Figure 21.
Polymer yield versus reactor pressure, confirming first order propagation order at high ethylene pressure.

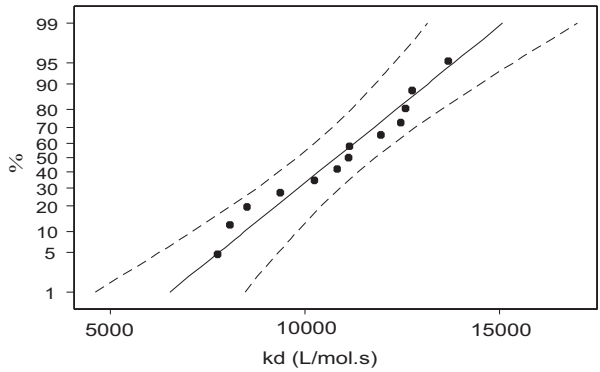

Figure 22.
Normal probability plot for k_d with 95% confidence limits.

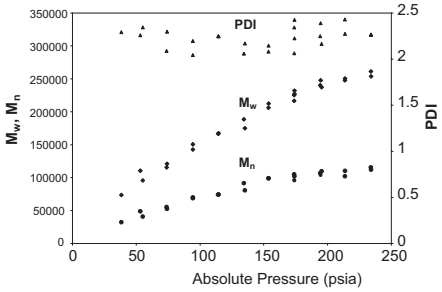

Figure 23.
Variation of M_n, M_w and *PDI* with polymerization pressure for ethylene polymerization with CGC-Ti.

the experimental data described in Figure 19 to 21.

Following a similar approach to the one used above for $Et(Ind)_2ZrCl_2$, the k_d was estimated to be $10800 \pm 1160\,L \cdot mol^{-1} \cdot s^{-1}$ (95% confidence interval). Its normal probability plot is shown in Figure 22.

Figure 23 shows how the M_n, M_w and *PDI* of polyethylene made with CGC-Ti vary with polymerization pressure. The *PDI* remains practically constant in all polymerizations, with values in a narrow range between 2 and 2.5, as theoretically expected for a single-site catalyst. Both M_n and M_w initially increase with polymerization pressure and then tend to constant values, which is consistent with a mechanism controlled by transfer to monomer.

Conclusions

The knowledge of the detailed polymerization kinetics or olefins with metallocene catalysts is essential for process scale-up and optimization, as well as for the development of products with new properties, especially when more than one metallocene catalyst is being used in the same reactor or when a single metallocene catalyst is used in a series of reactors operated at different conditions.

We have developed and applied a systematic methodology to determine the leading polymerization kinetic parameters for the solution polymerization of ethylene with rac-$Et(Ind)_2ZrCl_2$/MAO and (CGC-Ti)/MAO in a semi-batch reactor at 120 °C under different monomer pressures and catalyst concentrations. Ethylene polymerization with rac-$Et(Ind)_2ZrCl_2$/MAO follow the classic ''textbook'' first polymerization and catalyst deactivation kinetics. However, ethylene polymerization with (CGC-Ti)/MAO is described with

second order kinetics for catalyst decay and the order of polymerization changes from 2 to 1 with increasing ethylene pressure. To the best of our knowledge, this is the first time this behaviour is reported systematically for this catalyst system.

[1] J. D. Kim, J. B. P. Soares, G. L. Rempel, *Macromol. Rapid Commun.* **1998**, *19*, 197.
[2] J. D. Kim, J. B. P. Soares, *Macromol. Rapid Commun.* **1999**, *20*, 347.
[3] J. B. P. Soares, *Macromol. Mater Eng.* **2004**, *289*, 70.
[4] A. H. Dekmezian, P. Jiang, J. B. P. Soares, C. A. Garcia-Franco, W. Weng, H. Fruitwala, T. Sun, D. M. Sarzotti, *Macromolecules* **2002**, *35*, 9586.
[5] S. Mehdiabadi, J. B. P. Soares, A. H. Dekmezian, *Macromol. React. Eng.* **2008**, *2*, 37.
[6] V. C. Gibson, *Science* **2006**, *312*, 703.
[7] J. B. P. Soares, J. D. Kim, *J. Polym. Sci.: Part A: Polym. Chem.* **2000**, *38*, 1408.
[8] D. C. Montgomery, *Design and Analysis of Experiments*, 6th edition, John Wiley & Sons, New York 2005.
[9] L. S. Lee, H. J. Ou, H. L. Hsu, *Fluid Phase Equilibria* **2005**, *231*, 221.
[10] M. J. Ystenes, *J. Catal.* **1991**, *129*, 383.

